# COMPARATIVE ANALYSIS OF GRADED-INDEX AND STEP-INDEX OPTICAL FIBERS FOR STED MICROSCOPY

O. V. ANGELSKY, P. P. MAKSYMIAK, S. P. SHCHUKIN \*

Yuriy Fedkovych Chernivtsi National University, Department of Correlation Optics, 2 Kotsiubynskoho St., Chernivtsi, 58012, Ukraine \*Corresponding author: shchukin.serhii@chnu.edu.ua

Received: 23.10.2025

**Abstract.** Stimulated Emission Depletion (STED) microscopy is a super-resolution technique that uses structured light to break through the diffraction limit of traditional optical microscopy. A key part of STED is producing and delivering a donut-shaped depletion beam, typically achieved using optical vortex modes. This paper compares two types of optical fibers, step-index and parabolic graded-index (GRIN) fibers, in their ability to support and deliver the specific mode profiles needed for STED, such as Gaussian-like and vortex beams. Step-index fibers are simpler but have higher intermodal dispersion, modal degeneracy, and are more sensitive to perturbations. In contrast, GRIN fibers reduce modal dispersion, enhance mode stability, and improve spatial confinement because of their smooth refractive index profile. By constructing and analyzing mode field intensity distributions for specific fiber parameters, we demonstrate that GRIN fibers more effectively support dual-mode propagation and stable beam delivery for excitation and depletion wavelengths. These traits make them more suitable for compact, fiber-integrated STED microscopy systems. The findings aid in selecting and optimizing fibers for high-resolution imaging applications.

Keywords: optical fibers, optical vortices, LP modes, STED microscopy

UDC: 621.372: 535.38: 621.373

DOI: 10.3116/16091833/Ukr.J.Phys.Opt.2026.01027

This work is licensed under the Creative Commons Attribution International License (CC BY 4.0).

## 1.Introduction

Stimulated Emission Depletion (STED) microscopy is a super-resolution imaging method that exceeds the diffraction limit by spatially depleting fluorescence in targeted regions using a shaped depletion beam, usually a vortex beam with a central intensity null [1,2]. The effectiveness of STED microscopy heavily relies on the beam quality and stability of this depletion beam, which must sustain a high-contrast donut shape to restrict fluorescence to sub-diffraction volumes.

In traditional setups, vortex beams are generated using free-space optical components such as spatial light modulators (SLMs), spiral phase plates, or q-plates [3,4]. However, these components are bulky, sensitive to alignment, and not suitable for integration into compact or in vivo systems. To overcome these limitations, optical fibers, which can guide light over long distances with high spatial coherence, are increasingly explored as platforms for generating and delivering structured light beams for STED microscopy [5,6]. Specifically, few-mode fibers, photonic crystal fibers, and specialty fibers with azimuthally symmetric refractive index profiles that support orbital angular momentum (OAM) modes are commonly used for vortex beam generation and delivery in fiber-based STED systems [2].

The effectiveness of fiber-based STED systems depends on the fiber's ability to support stable guided modes, particularly those capable of carrying orbital angular momentum (OAM), such as linearly polarized (LP) modes and their superpositions. Among these, the LP

mode family is often used to generate optical vortices needed for donut-shaped depletion beams. A comparison of different optical fiber types, including graded-index fibers with a parabolic refractive index profile and step-index fibers, within the framework of the weakly guiding approximation is therefore essential to assess their suitability for providing the mode stability and beam shaping required for high-resolution STED imaging.

Step-index fibers are characterized by a sharp refractive index contrast between the core and cladding. This straightforward structure supports multiple *LP* modes depending on the core diameter and numerical aperture. In weakly guiding step-index fibers, the small refractive index difference allows the use of scalar approximation and *LP* mode classification [7]. While weakly guiding fibers provide analytical simplicity and well-understood mode structures, they are susceptible to modal degeneracy. Specifically, near-degenerate HE, EH, TE, and TM modes can couple under perturbations such as bending or index fluctuations, causing degradation of the vortex beam profile [8]. Additionally, step-index fibers show relatively high intermodal dispersion, limiting their ability to preserve coherent superpositions of modes necessary for high-purity vortex generation. This creates challenges for ultrafast STED applications, where pulse broadening and modal instability can impair image resolution. Although mode conversion techniques like long-period gratings or mode-selective couplers can excite specific *LP* modes, their effectiveness is limited by the fiber's inherent modal instability.

Graded-index (GRIN) fibers provide solutions to many of these challenges. In GRIN fibers, the refractive index gradually decreases from the center of the core to the cladding, often following a parabolic profile. This index gradient causes light rays to bend continuously toward the fiber axis, resulting in periodic self-focusing and reduced modal dispersion [7]. Consequently, GRIN fibers enable stable, low-loss propagation of multiple modes over longer distances, even under bending or mechanical stress [9,10]. Notably, GRIN fibers offer improved modal separation compared to step-index designs. This reduces intermodal coupling and helps maintain the spatial phase structure of vortex beams. For STED microscopy, this results in a more robust and stable donut-shaped depletion beam at the fiber output. When combined with appropriate mode conversion components such as fiber gratings, tapers, or photonic lanterns, GRIN fibers can generate high-purity OAM modes with extinction ratios >17.5 dB and mode conversion efficiencies over 98% [9]. Additionally, the parabolic index profile minimizes differential group delay between modes, preserving temporal coherence in pulsed systems - an essential feature for time-gated or femtosecond-pulsed STED applications. GRIN fibers are also mechanically flexible and compatible with compact imaging setups, making them suitable candidates for endoscopic and in vivo STED microscopy.

The process of generating vortex beams in fiber optics usually involves coherently exciting specific  $\mathit{LP}$  modes with a  $\pi/2$  phase difference to create azimuthally varying phase profiles. These  $\mathit{LP}$  modes serve as approximations to the fiber's true vector modes, which are the true eigenmodes characterized by well-defined polarization and spatial field distributions. By precisely controlling the amplitude and phase relationships between these vector modes, it becomes possible to produce stable vortex beams with specific orbital angular momentum properties for advanced uses like STED microscopy. This approach depends on accurate mode excitation and minimal coupling between modes during propagation.

GRIN fibers enable more reliable generation of such beams due to their stable mode profiles and reduced modal dispersion. Analytical descriptions based on Laguerre-Gaussian (LG) modes can be used to model the evolution of vortex beams within parabolic index fibers [11]. Recent theoretical research has also identified "harmonic motion modes" in GRIN fibers, which exhibit breathing or rotating intensity patterns that may influence vortex beam behavior during propagation [12].

While weakly guiding fibers allow for easier analysis, their limited modal separation and greater sensitivity to disturbances make them less suitable for high-resolution STED systems without additional stabilization mechanisms. Step-index fibers provide moderate performance but experience higher intermodal dispersion. In contrast, GRIN fibers present a balanced solution, delivering high beam fidelity, compact integration, and compatibility with both continuous-wave and pulsed STED modes.

This work compares GRIN fibers, with their parabolic refractive index profile, and step-index fibers for use in STED microscopy. Using theoretical modeling and analysis of existing experimental data [9], we aim to evaluate the trade-offs between fiber types and offer guidance for optimizing fiber-based STED systems. The goal is to identify the strengths and weaknesses of GRIN and step-index fibers in terms of optical performance and practical integration, helping optimize fiber-based STED implementations.

# 2. Fundamentals of STED microscopy

STED microscopy is a revolutionary imaging technique that surpasses the classical diffraction limit of optical microscopy, allowing researchers to observe structures at the nanoscale in biological and material samples. First proposed theoretically by Stefan W. Hell and Jan Wichmann in 1994 [1] and experimentally achieved in the late 1990s, STED microscopy established the foundation for super-resolution imaging, earning Hell a share of the 2014 Nobel Prize in Chemistry.

At the core of STED microscopy is the idea of spatially controlling the fluorescence emission of fluorophores to reduce the effective size of the point spread function (PSF), which in traditional microscopy is limited by diffraction to roughly half the wavelength of light (~200–250 nm for visible wavelengths) [2]. According to Abbe's law, this limit is given by  $d = \lambda / 2NA$ , where  $\lambda$  is the wavelength and NA is the numerical aperture of the imaging system. STED microscopy overcomes this limitation by using a second, precisely shaped laser beam to deplete fluorescence in specific regions of the excitation focal spot, thus sharpening the effective area from which fluorescence is detected. The STED technique involves at least two laser beams: one for excitation and another for depletion. The excitation beam, usually pulsed, excites fluorophores from the ground state to the excited state, just like in standard fluorescence microscopy. Nearly simultaneously or with a brief delay, a second laser beam, called the STED beam, is applied. This beam is tuned to a wavelength longer than the emission wavelength and is designed to induce stimulated emission in fluorophores, forcing them to return to the ground state without emitting a fluorescence photon. Importantly, the STED beam is spatially modulated, often into a donut shape with a zero-intensity center, so that only fluorophores at the very center of the excitation spot remain unaffected and can fluoresce. This selective suppression of fluorescence sharpens the focal volume, effectively narrowing the PSF and improving resolution.

The resolution improvement in STED microscopy is not binary but rather depends on the intensity of the depletion beam. The effective resolution  $d_{sted}$  scales inversely with the square root of the STED beam intensity I, following the equation:

$$d_{sted} = \frac{d_0}{\sqrt{1 + I/I_s}},\tag{1}$$

where  $d_0$  is the diffraction-limited resolution and  $I_s$  is the saturation intensity required to reduce fluorescence by 50%. Therefore, in theory, infinitely high resolution can be achieved with infinitely high STED intensity. However, practical limits such as photobleaching, phototoxicity, and optical aberrations restrict the usable depletion power [2].

STED microscopy offers several key advantages. It provides real-time super-resolution imaging with spatial resolutions as fine as 20–30 nm, allowing visualization of subcellular structures and molecular distributions that are beyond the reach of diffraction-limited techniques. Unlike some other super-resolution methods, STED does not depend on stochastic processes or post-processing algorithms; its resolution is determined optically during image acquisition. Additionally, STED is compatible with multicolor imaging, permitting the simultaneous observation of different biological targets with nanoscale precision.

However, STED microscopy faces certain challenges. The requirement for high depletion intensities can cause photobleaching and phototoxic effects, mainly in live-cell imaging. Aligning and calibrating the excitation and STED beams are technically complex tasks, and the system costs are much higher than traditional confocal or widefield microscopes. Additionally, the performance of STED is affected by sample-induced aberrations, especially in thick or heterogeneous samples, which can distort beam profiles and reduce resolution. These issues can be addressed with adaptive optics and wavefront correction techniques.

To support ongoing development, research continues into better fluorophores, more efficient beam shaping techniques, and compact STED-compatible fiber optics, such as GRIN fibers. GRIN fibers are especially promising for delivering shaped beams over short distances, potentially enabling miniaturized or endoscopic STED systems [10].

In summary, STED microscopy is a powerful and versatile method for super-resolution imaging, capable of resolving structures well beyond the diffraction limit by utilizing stimulated emission and spatial light control. Although technical challenges still exist, ongoing innovations in optics, laser technology, and probe design continue to expand the reach and accessibility of STED, opening new possibilities in nanoscale imaging across biology, medicine, and materials science. In this context, the role of optical vortices – structured light fields carrying orbital angular momentum – is particularly important. These vortices, especially when generated and transmitted through optical fibers, enhance the precision and control of the depletion beam profile in STED systems [9]. Their inherent phase singularity and doughnut-shaped intensity distribution make them ideal for confining fluorescence within sub-diffraction volumes. The stability and mode structure of optical vortices in fiber systems are essential for maintaining the beam quality needed for effective resolution improvement. Advances in fiber design, such as vortex-supporting photonic crystal fibers and few-mode fibers, have further increased the robustness and fidelity of vortex beam transmission, enabling more stable and efficient implementation of vortex-

based depletion techniques in practical STED microscopy.

The following section provides a comparative analysis of GRIN fibers with various transverse refractive index profiles, emphasizing their efficiency in supporting optimal beam shaping and stability, which are critical for high-performance STED microscopy.

# 3. Graded-index vs. step-index fibers for STED microscopy

GRIN optical fibers have unique propagation properties because of their radially varying refractive index profile. A major feature of these fibers is the support for scalar *LP* modes, which approximate the true vector modes under weak guidance conditions. In such fibers, the refractive index of the core (*n*) changes radially, being highest at the center and gradually decreasing toward the cladding. Under the weakly guiding approximation (i.e., when the core-cladding index difference is small), the entire vector wave equations simplify to scalar wave equations. In this regime, solutions to the wave equation are well approximated by *LP* modes [7]. These *LP* modes are classified by radial and azimuthal mode numbers and are crucial for understanding light propagation in multimode GRIN fibers. A common refractive index profile for a GRIN fiber is the one given by:

$$n(r) = n_0 \left[ 1 - 2\Delta \left( \frac{r}{\rho} \right)^g \right]^{1/2}, \quad r < \rho,$$

$$n(r) = n_{cl} \qquad r > \rho$$
(2)

where  $\Delta = \frac{1}{2}(1-n_{cl}^2/n_0^2)$  contains  $n_0$  that is the maximum refractive index in the fiber, and  $n_{cl}$  is the cladding index,  $\rho$  is the core radius, g – profile exponent. A special case of GRIN fibers occurs when the refractive index follows a parabolic profile with respect to radius r, which happens when the profile exponent g=2 in Eq. (2). For a fiber with a step refractive index profile, Eq. (2) changes to  $n(r)=n_0$  when  $r<\rho$  and  $n(r)=n_{cl}$  when  $r>\rho$ .

#### 3.1. Basic equations

When vector and polarization effects are neglected, the electric field E (assuming time-harmonic dependence  $e^{-i\omega t}$  and wave propagation along the fiber axis  $e^{i\beta z}$ ) in the transverse plane of the fiber (i.e., the cross-section) satisfies the scalar Helmholtz equation:

$$\Delta_{\perp} E + (k^2 n^2 - \beta^2) E = 0, \qquad (3)$$

where  $k=2\pi/\lambda$  is the free-space wavenumber,  $\lambda$  is the wavelength,  $\beta$  is the propagation constant along the fiber axis. Solutions of Eq. (3) yield the guided modes of the fiber along with their respective propagation constants  $\beta$ . In the cylindrical geometry of an axially symmetric fiber with  $(r,\varphi,z)$  coordinates, we seek propagating solutions of separable form  $E \otimes R(r)e^{il\varphi}$ , where R(r) is the radial part, l is the azimuthal mode number (integer). Substituting the last expression into Eq. (3) and making a substitution  $\psi=r^{1/2}R(r)$ , for the dimensionless variable  $y=r/\rho$ , we get:

$$-\frac{d^2\psi}{dy^2} + \frac{l^2 - 1/4}{y^2}\psi - \rho^2(n^2k^2 - \beta^2)\psi = 0.$$
 (4)

Next, following [7], we will define  $V = \rho k n_0 \sqrt{2\Delta}$  (the V-number or normalized frequency of

an optical fiber), and  $U = \rho \sqrt{k^2 n_0^2 - \beta^2}$  (normalized propagation constant). If we introduce the numerical aperture of the fiber  $NA = \sqrt{n_0^2 - n_{cl}^2}$ , then the *V*-number can be expressed as  $V = \rho k NA$ . Using this notation, the Eq. (4) can be rewritten as

$$-\frac{d^2\psi}{dy^2} + \frac{(l^2 - 1/4)}{y^2}\psi + V^2y^g\psi = U^2\psi, \qquad y < 1,$$
 (5)

where Eq. (2) is used. If y>1, then a replacement  $y^g\to 1$  should be made. This equation is analogous to the one-dimensional Schrödinger equation, whose potential includes a term (the second term in Eq. (5)) due to the circular shape of the fiber [13]. This term is analogous to the "centrifugal potential" used in similar quantum mechanical considerations. The expression  $U^2$  plays the role of energy, the value of which determines the propagation constant  $\beta$ . As with quantum mechanics, solutions of the wave Eq. (5) lead to a discrete set of bound modes and a continuum of radiation modes.

## 3.2. Parabolic index fiber

Consider a GRIN fiber with a refractive index profile exponent g=2, corresponding to a parabolic refractive index distribution. This parabolic profile leads to a wave equation that is mathematically analogous to that of a two-dimensional isotropic quantum harmonic oscillator [13]. Indeed, after changing the variable  $x = V^{1/2}y$ , Eq. (5) can be rewritten as

$$\left[ -\frac{1}{2} \frac{d^2}{dx^2} + \frac{1}{2} \left( x^2 + \frac{(l^2 - 1/4)}{x^2} \right) \right] \psi = \frac{U^2}{2V} \psi , \tag{6}$$

This equation has a set of eigenfunctions and eigenvalues that define the mode spectrum of the GRIN optical fiber [7] as

$$\psi_{lm} = Nx^{|l| + \frac{1}{2}e^{-\frac{x^2}{2}} L_m^{|l|}(x^2), \tag{7a}$$

and

$$\frac{U_{lm}^2}{2V} = 2m + |l| + 1, (7b)$$

where  $L_m^{|I|}(x^2)$  is the associated Laguerre polynomial, m is the radial mode number (non-negative integer), and N is the normalization constant. In weakly guiding parabolic fibers, the propagation constant, as follows from the definition of  $U_{lm} = \rho \sqrt{k^2 n_0^2 - \beta_{lm}^2}$  and Eq. (7b), is given by

$$\beta_{lm} \cong kn_0 \left( 1 - 2\Delta \frac{2m + |l| + 1}{V} \right). \tag{8}$$

Thus, the propagation constants in a parabolic refractive-index fiber form an equidistant sequence of eigenstates, Eq. (6). Each state is characterized by two numbers, m and l. But the propagation constants  $\beta_{lm}$  depend only on the combination N=2m+|l|. Each value  $N\geq 2$  can be realized by several combinations of values m and l; therefore, the corresponding modes with values  $N\geq 2$  are degenerate. Thus, the superposition of these modes can form stable structures, since they have equal propagation constants. However, the existence of these modes can only be asserted if the phase of the superposition is proportional to  $l\varphi$ . Thus, if we take a pair (l,m), then in weakly guiding step-index optical

fibers combinations (l,m) and (l+2,m) form an LP mode. In contrast, in a parabolic refractive index fiber it is necessary to choose (l,m) and (l+2,m-1).

Due to the weak guidance approximation (small index contrast), the actual fiber modes (HE, EH, TE, TM) can be approximated as  $LP_{lm}$ . Among these, certain modes possess phase singularities and azimuthal phase structures characteristic of optical vortices, making parabolic index fibers naturally suited for guiding light with OAM. In standard step-index fibers, which have a uniform core refractive index and a sudden drop at the cladding, the lowest order supported mode is typically labeled  $LP_{01}$ . This mode approximates the exact vector mode  $HE_{11}$  and is often referred to as the fundamental mode in such fibers [7]. Importantly, the  $LP_{00}$  mode does not exist in step-index fibers because it does not satisfy the necessary boundary conditions imposed by the abrupt refractive index change at the core-cladding interface.

However, in fibers with a graded refractive index, particularly those with a parabolic index profile, the situation is different. In these fibers, the  $LP_{00}$  mode is the fundamental mode, characterized by the absence of orbital angular momentum and a transverse profile analogous to that of a Gaussian beam. In contrast, modes like  $LP_{10}$ ,  $LP_{11}$ ,  $LP_{21}$ , and higher-order modes support vortex solutions with |I|=1,2,..., corresponding to increasingly complex helical phase fronts and ring-shaped intensity profiles. The  $LP_{10}$  mode, for instance, exhibits a donut-shaped intensity distribution with a central null, a hallmark of optical vortex beams. However, any deviation from this symmetry, such as fiber bending, manufacturing imperfections, or intentional index modulation, can lift the degeneracy between +I and -I modes and cause mode coupling. This is a critical consideration in the design of OAM-based communication systems, where mode purity is essential for minimizing cross-talk. Thus, parabolic-index optical fibers provide a natural environment for the propagation of LP modes, many of which exhibit vortex characteristics due to their azimuthal phase dependence.

In STED microscopy, one desires the coexistence of a central Gaussian (or near-Gaussian) excitation beam and a coaxial donut-depletion beam. A fiber capable of guiding both the fundamental  $LP_{00}$  mode and a higher-order vortex LP mode (such as  $LP_{10}$  or  $LP_{11}$ ) is highly advantageous. The fiber must enable mode conversion (or multiplexing) from a conventional single-mode excitation input to the appropriate spatial modes, and thereafter preserve the mode purity and spatial alignment over the propagation length. Parabolic refractive index fibers, a specific type of GRIN fiber, offer distinct advantages for STED microscopy due to their tailored modal and dispersion properties. In these fibers, the  $LP_{00}$  mode exhibits a Gaussian-like intensity profile, ideal for delivering the excitation beam with high spatial fidelity. Simultaneously, the  $LP_{10}$  mode displays a doughnut-shaped intensity distribution, which is perfectly suited for generating the depletion ring required for STED resolution enhancement. The parabolic refractive index profile ensures that light rays follow sinusoidal trajectories, thereby significantly reducing intermodal dispersion. As a result, both excitation and depletion beams can propagate through the fiber and arrive at the output end nearly simultaneously and with minimal distortion. This temporal and spatial coherence is critical for maintaining the precise overlap required for effective STED imaging, making parabolic GRIN fibers particularly well-suited for compact and fiber-based super-resolution systems.

Thus, to create efficient fiber-based STED systems, one can limit oneself to just two modes ( $\mathit{LP}_{00}$  and  $\mathit{LP}_{10}$ ) that are excited and propagate in the system simultaneously. Table 1 presents the main parameters that define a dual-mode configuration in fiber-based STED microscopy systems. In such systems, the reliable and distortion-free delivery of both the excitation and depletion beams, often launched in distinct spatial modes (e.g.,  $\mathit{LP}_{00}$  and  $\mathit{LP}_{10}$ ) and at significantly different wavelengths, requires careful optimization of the fiber properties. Specifically, parameters such as core diameter, numerical aperture, refractive index profile, mode-field overlap, and intermodal dispersion must be precisely controlled to ensure stable and high-fidelity beam propagation. As shown in Table 1 (see, for example, [6, 9]), these parameters are critical for enabling effective depletion beam shaping and spatial-temporal alignment, which are essential for achieving super-resolution in STED microscopy.

**Table 1.** Key fiber parameters for STED applications.

| Parameter  | Typical Requirement  | Purpose                                       |
|--|--|---|
| Core radius, $ ho$   | 1.5–3 μm (single-mode), or larger for few-mode fibers                | Control modal content                         |
| Numerical Aperture ( $NA$ ) $NA = \sqrt{n_0^2 - n_{cl}^2}$ | 0.1–0.3 (single-mode), up to 0.5 for few-mode                        | Affects resolution and mode size              |
| Index profile  | Parabolic (graded index) or step-<br>index                           | Supports well-defined <i>LP</i> and OAM modes |
| Mode support   | $LP_{00}$ and $LP_{10}$ (or OAM ±1 modes)                            | Gaussian + donut beam<br>delivery             |
| $V$ -number ( $V$ ) $V = \rho kNA$                         | $\sim$ 2.5–4.0 to support 2-3 mode                                   | Controlled by core size and <i>NA</i>         |
| Wavelengths, $\lambda$                                     | Excitation ( $\sim$ 488–594 nm), STED depletion ( $\sim$ 750–800 nm) | Fibers must support both wavelengths          |
| Birefringence  | Low or polarization-maintaining                                      | Stable vortex delivery                        |
| Length   | Short (~10 cm to a few meters)                                       | To avoid mode mixing                          |
| Mode purity  | High   | Critical for donut shape in depletion beam    |

The core diameter is one of the most critical design aspects. For single-mode operation at the excitation wavelength (typically 488–594 nm), a core diameter of 3–6  $\mu$ m is common. For few-mode fibers that support both the fundamental and higher-order modes (or their OAM equivalents), a slightly larger core is needed to ensure clean dual-mode operation while minimizing unwanted mode mixing. The numerical aperture determines the range of supported modes and influences both mode confinement and spatial resolution. Single-mode fibers typically use NA values between 0.1 and 0.3, while higher NA up to 0.5 may be employed in few-mode fibers to support additional mode families. A larger NA enables tighter beam focusing at the output, which is beneficial for resolution but may increase sensitivity to alignment and modal dispersion. The index profile, whether parabolic (graded-index) or step-index, plays a fundamental role in mode propagation. Parabolic index profiles are often preferred in STED

applications due to their low intermodal dispersion and more stable support for spatially distinct LP modes or OAM states, which are required to generate Gaussian (excitation) and donut (depletion) beam shapes. To ensure selective support of only the desired modes, the fiber V-number must be carefully controlled. A V-number in the range of 2.5 to 4.0 is typically sufficient to support exactly two or three modes enabling dual-mode delivery while avoiding higher-order mode interference. The V-number depends on the core diameter, NA, and operating wavelength. Since STED requires simultaneous propagation at two widely spaced wavelengths – typically  $\sim$ 488–594 nm for excitation and  $\sim$ 750–800 nm for depletion – the fiber must support the correct modal structure at both wavelengths. This dual-wavelength operation often imposes constraints on core size and index contrast to maintain mode selectivity.

Birefringence is another critical factor. Low-birefringence fibers are acceptable when polarization is not tightly controlled, but for vortex beams (e.g., OAM modes), polarization-maintaining (PM) fibers are preferred to ensure stable beam shapes, especially for depletion, where a precise phase structure (e.g., a vortex or donut) is required. The fiber length must also be minimized, typically kept short ( $\sim$ 10 cm to a few meters), to prevent differential mode delay, modal dispersion, and unwanted mode coupling that could distort the spatial beam profiles. Finally, mode purity is paramount, particularly for the depletion beam delivered in the  $LP_{10}$  or OAM mode. Any contamination from the fundamental mode can fill in the central null of the donut beam, significantly reducing STED resolution. High mode purity is thus essential for maintaining the sharp spatial profile required for efficient fluorescence depletion. Together, these parameters define the operating window for fibers used in STED microscopy and guide the selection or custom fabrication of fibers tailored for high-resolution, dual-mode, dual-wavelength beam delivery.

Fig. 1 illustrates the transverse intensity profiles of two *LP* modes supported by the optical fiber. The left panel shows the intensity distribution of the STED depletion mode, calculated at 775 nm, which exhibits a characteristic doughnut-shaped profile due to its nonzero azimuthal

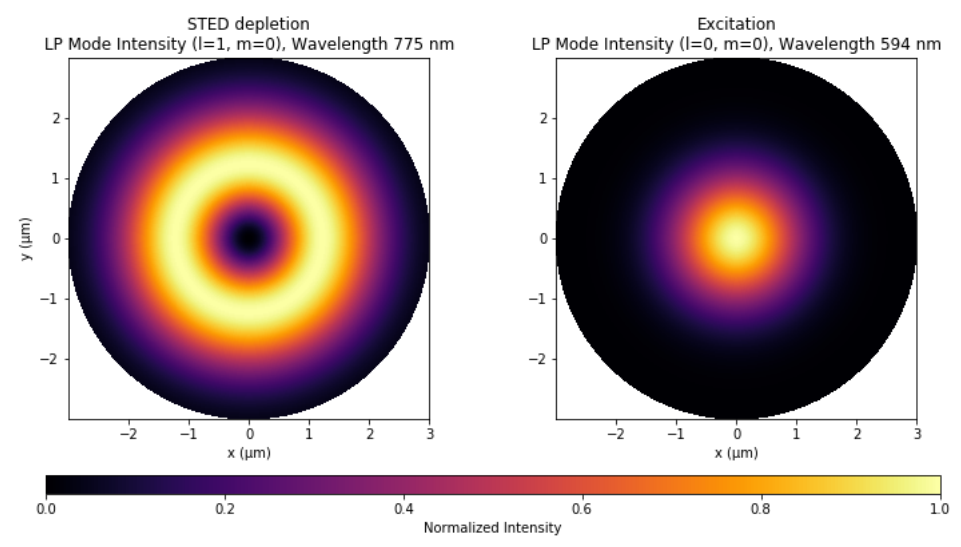


**Fig. 1.** Transverse intensity distributions of LP modes in the parabolic refractive index fiber: (left) STED depletion mode  $LP_{10}$  at 775 nm, (right) excitation mode  $LP_{00}$  at 594 nm. The core index is  $n_0$ =1.48, the core radius is  $\rho$  = 3 µm,  $\Delta$  = 0.01342. The plots show normalized intensity  $R(r)^2$  in the (x, y) plane. A common color scale is used for both modes.

index. The right panel displays the excitation mode  $LP_{00}$  at 594 nm, corresponding to the fundamental Gaussian-like intensity distribution. Both profiles are computed using the Laguerre-Gaussian approximation (7a) and are plotted in the transverse (x,y) plane with a common color scale representing the optical intensity  $R(r)^2$  normalized to its maximum value. Note that the actual intensity is proportional to the square of the field, which includes  $\sin(l\varphi)$  or  $\cos(l\varphi)$  angular components that give rise to lobes in the azimuthal direction. However, since our focus is on the radial intensity dependence for STED applications, we omit the angular dependence here for clarity. These spatial mode patterns are critical for understanding the overlap between excitation and depletion beams in STED microscopy applications using fiber delivery.

In a graded-index fiber with a parabolic refractive index profile, the number of guided modes depends on the normalized frequency parameter V, just as in a step-index fiber, but the scaling is different. In this case, the approximate number of guided modes (including both polarizations) is  $V^2/4$ . In our example, the value of the parameter V is 5.897 at 775 nm, so the approximate number of modes does not exceed 4 for one polarization. If we classify the modes by their eigenvalues according to Eq. (7b), then the chain of eigenvalues is:  $U_{00}^2 = 2V$ ,  $U_{10}^2 = 4V$ ,  $U_{01}^2 = 6V$ ,  $U_{20}^2 = 6V$ . Thus, the higher order modes are degenerate, they have the same propagation constants and, therefore, the same phase velocities. The  $LP_{10}$  mode forms a ring-shaped pattern suitable for STED beam shaping, while the  $LP_{00}$  mode exhibits a central maximum typical for efficient excitation.

### 3.3. Step-index fiber

It is useful to compare the intensity distribution patterns in parabolic-index and step-index fibers under the same parameters in the weakly guiding approximation. Fig. 2 shows the normalized intensity distribution of the  $LP_{11}$  and  $LP_{01}$  modes propagating in a weakly guiding step-index fiber.

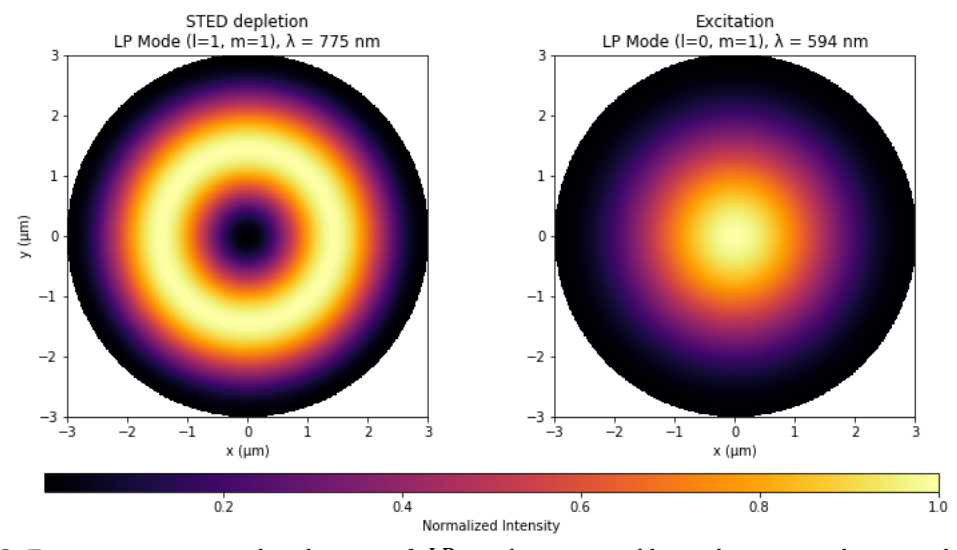


**Fig. 2.** Transverse intensity distributions of LP modes in a weakly guiding step-index optical fiber: (left) STED depletion mode  $LP_{11}$  at 775 nm, (right) excitation mode  $LP_{01}$  at 594 nm. The core index  $n_0$ =1.48, the core radius is  $\rho$  = 3 µm,  $\Delta$  = 0.01342. The plots show normalized intensity  $R(r)^2$  in the (x,y) plane. A common color scale is used for both modes.

The core radius is set to 3  $\mu$ m, and the core refractive index is 1.48. The relative index difference,  $\Delta$ , is 0.01342, consistent with weakly guiding fibers where LP modes are valid approximations. Two wavelengths are considered: 594 nm for excitation and 775 nm for depletion. These correspond to typical choices in STED microscopy, where a shorter wavelength excites fluorescence and a longer wavelength quenches it via stimulated emission. At 594 nm, the V-number is approximately 7.69, while at 775 nm it is about 5.9. Both values are well above the single-mode cutoff of 2.405, indicating that the fiber supports many LP modes and operates in a highly multimode regime. The  $LP_{01}$  mode, with azimuthal index I=0 and radial index I=1, represents the fundamental mode with a single intensity peak at the center of the fiber. It is rotationally symmetric and ideal for focusing excitation light at the core center. The  $LP_{11}$  mode, with I=1 and I=1, exhibits a ring-shaped intensity profile due to its angular dependence.

The electric fields of these modes are derived from the scalar wave equation in cylindrical coordinates. Inside the fiber core, the fields are described by Bessel functions of the first kind,  $J_l(U_{lm}r/\rho)$ , and in the cladding by modified Bessel functions of the second kind,  $K_l(W_{lm}r/\rho)$ . The radial propagation constants  $U_{lm}$  are actually determined from the boundary conditions that ensure continuity of the field and its derivative at the corecladding interface, and the cladding decay constants  $W_{lm}$  follow from  $W_{lm} = \sqrt{V^2 - U_{lm}^2}$  [7]. The fields are then squared to obtain normalized intensity profiles. As expected, the  $LP_{01}$  mode displays a bright, centralized peak, while the  $LP_{11}$  mode shows a dark center surrounded by a bright ring, consistent with its doughnut shape.

These results illustrate how carefully selected LP modes can be used to shape light fields within a fiber, enabling advanced microscopy techniques. By using the  $LP_{01}$  mode for excitation and  $LP_{11}$  for depletion, spatial separation of the excitation and quenching regions is achieved, mimicking the fundamental principle of STED. This approach demonstrates that a multimode fiber, despite its complexity, can be exploited to deliver structured light profiles without requiring complex free-space optics.

In conclusion, the calculations presented confirm the feasibility of generating the desired mode profiles in a step-index fiber. The  $LP_{01}$  and  $LP_{11}$  modes exhibit complementary spatial intensity distributions, suitable for excitation and depletion in STED microscopy. The field distributions were computed using standard analytical expressions for LP modes derived from the scalar wave equation under the weakly guiding approximation. This approach can be readily extended to other mode combinations or fiber geometries and may be useful in fiber-based super-resolution imaging or integrated photonic systems.

## 3.4. Fiber choice in STED microscopy: A comparative approach

The choice between these two fiber types depends on the specific requirements of the application. The most important selection criteria are summarized in Table 2.

Parabolic-index fibers offer significant advantages in STED microscopy due to their gradually varying refractive-index profile. This smooth transition enables superior mode shaping, tightly confining the excitation beam and thereby enhancing spatial resolution. Additionally, the parabolic profile supports a depletion beam with a well-defined central null, a critical feature for effective fluorescence suppression. This results in better spatial selectivity between the excitation and depletion regions, ultimately improving image sharpness and contrast.

**Table 2.** Comparative analysis.

| Feature                  | Parabolic Index Fiber  | Step-Index Fiber   |
|--------------------------|--|--|
| STED Mode (775 nm)       | More symmetric, smoother ring, stronger central null               | Similar doughnut shape,<br>but less uniform and with<br>broader ring |
| Excitation Mode (594 nm) | Sharply focused, narrower<br>Gaussian spot                         | Slightly broader and less confined center peak                       |
| Mode confinement         | Better spatial confinement, especially in excitation               | Less confinement, broader intensity distribution                     |
| Beam overlap             | Stronger spatial separation between excitation and depletion modes | More overlap due to broader excitation profile                       |
| Ideal for STED?          | Yes – tighter focus and cleaner depletion ring improve resolution  | Less optimal – broader<br>modes reduce STED<br>efficiency            |

In contrast, step-index fibers present certain limitations. The abrupt change in refractive index reduces control over the modal field shape, often resulting in a broader excitation mode that can unintentionally excite fluorophores outside the depletion null. Furthermore, the STED beam formed in such fibers tends to be more ring-shaped, with less contrast between the center and periphery, thereby diminishing the effectiveness of fluorescence suppression.

In summary, both fiber types can support the modes required for STED microscopy. Still, the parabolic-index fiber provides smoother mode profiles and improved spatial separation between excitation and depletion beams. Step-index fibers, while more straightforward and more robust, exhibit broader mode distributions that may limit ultimate resolution. Overall, the parabolic design provides better control over field confinement and mode overlap, making it more favorable for achieving high-resolution fiber-based STED imaging.

#### 4. Conclusions

This study presents a comparison between step-index and GRIN optical fibers regarding their suitability for delivering structured light beams, specifically Gaussian and donutshaped modes, required for high-performance STED microscopy. While step-index fibers offer simplicity and support for multiple modes under the weakly guiding approximation, they suffer from limitations such as high intermodal dispersion, modal degeneracy, and sensitivity to perturbations, all of which can degrade the spatial integrity of the depletion beam and reduce imaging resolution. In contrast, GRIN fibers, particularly those with a parabolic refractive index profile, demonstrate superior modal stability, reduced intermodal dispersion, and improved spatial separation between excitation and depletion beams. These characteristics enable more efficient generation and delivery of high-purity vortex beams, thereby enhancing the spatial and temporal coherence required for STED imaging. The ability of GRIN fibers to support stable LP and OAM modes, even under mechanical stress or bending, arises from their parabolic refractive index profile, which causes the modes to be strongly confined toward the fiber center. This central confinement reduces sensitivity to perturbations, maintaining well-defined mode shapes and spatial intensity distributions. Such intrinsic stability makes parabolic GRIN fibers highly advantageous for compact, integrated, and potentially in vivo STED microscopy systems, where robust and reproducible beam delivery is essential.

By examining the computed mode field distributions for the selected fibers, this work highlights the importance of proper fiber choice and configuration in optimizing STED performance. The results clearly indicate that parabolic-index GRIN fibers provide a more robust and scalable platform for fiber-based STED microscopy, paving the way for miniaturized super-resolution imaging systems that combine optical precision with mechanical flexibility.

**Funding.** This research was funded by the National Research Foundation of Ukraine, project No. 2025.06/0086 'Innovative Methods and Systems of Laser Communication in Turbulent Atmospheric Environments Based on Phase Singularities'.

Disclosures. The authors declare no conflicts of interest.

#### References

- Hell, S. W., & Wichmann, J. (1994). Breaking the diffraction resolution limit by stimulated emission: stimulatedemission-depletion fluorescence microscopy. Optics Letters, 19(11), 780-782.
- 2. Blom, H., & Widengren, J. (2017). Stimulated emission depletion microscopy. Chemical reviews, 117(11), 7377-7427.
- 3. Allen, L., Barnett, S. M., & Padgett, M. J. (2016). Optical angular momentum. CRC press.
- 4. Fu, S., & Gao, C. (2023). Optical vortex beams. Springer.
- Ma, M., Lian, Y., Wang, Y., & Lu, Z. (2021). Generation, transmission and application of orbital angular momentum in optical fiber: A review. Frontiers in Physics, 9, 773505.
- 6. Ramachandran, S., & Kristensen, P. (2013). Optical vortices in fiber. Nanophotonics, 2(5-6), 455-474.
- 7. Snyder, A. W., & Love, J. D. (1983). Optical waveguide theory (Vol. 175). London: Chapman and Hall.
- 8. Bozinovic, N., Yue, Y., Ren, Y., Tur, M., Kristensen, P., Huang, H., Willner, A.E. & Ramachandran, S. (2013). Terabit-scale orbital angular momentum mode division multiplexing in fibers. *Science*, *340*(6140), 1545-1548.
- 9. Yan, L., Kristensen, P., & Ramachandran, S. (2019). Vortex fibers for STED microscopy. APL Photonics, 4(2).
- 10. Heffernan, B. M., Meyer, S. A., Restrepo, D., Siemens, M. E., Gibson, E. A., & Gopinath, J. T. (2019). A fiber-coupled stimulated emission depletion microscope for bend-insensitive through-fiber imaging. *Scientific Reports*, *9*(1), 11137.
- 11. Khonina, S. N., Striletz, A. S., Kovalev, A. A., & Kotlyar, V. V. (2010, January). Propagation of laser vortex beams in a parabolic optical fiber. In *Optical Technologies for Telecommunications 2009* (Vol. 7523, pp. 82-93). SPIE.
- 12. Collado Hernández, A., Marroquín Gutiérrrez, F., & Rodríguez-Lara, B. M. (2024). Harmonic motion modes in parabolic GRIN fibers. *Optics Continuum*, *3*(6), 1025-1037.
- 13. Black, R. J., & Ankiewicz, A. (1985). Fiber-optic analogies with mechanics. American Journal of Physics, 53(6), 554-563.

Angelsky, O. V., Maksymiak, P. P., Shchukin, S. P. (2026). Comparative Analysis of Graded-Index and Step-Index Optical Fibers for STED Microscopy. *Ukrainian Journal of Physical Optics*, *27*(1), 01027–01039. doi: 10.3116/16091833/Ukr.J.Phys.Opt.2026.01027

Анотація. Мікроскопія на основі стимульованого випромінювання та пригнічення спонтанного випромінювання (STED) — це метод над роздільної здатності, який спирається на структуроване світло для подолання дифракційної межі звичайної оптичної мікроскопії. Критичною функцією STED є генерація та передача променя пригнічення у тороїдальній формі, що, зазвичай, досягається за допомогою оптичних вихрових мод. У цій статті порівнюються два типи оптичних волокон: волокна зі східчастим профілем показника заломлення та волокна з параболічним градієттним профілем показника заломлення (GRIN), щодо їхньої здатності підтримувати та передавати специфічні профілі мод, необхідні для STED, а саме гаусові та вихрові промені. Волокна зі східчастим профілем є простими, але їх недоліками є вища міжмодова дисперсія, модальне виродження та чутливості до збурень. Натомість волокна GRIN забезпечують зменшену модальну дисперсію, підвищену стабільність мод та покращене просторове обмеження завдяки плавному профілю показника заломлення. На основі побудови та аналізу розподілів інтенсивності мод для обраних параметрів волокон ми показуємо, що волокна GRIN більш ефективно підтримують одночасне поширення двох мод і стабільне доставляння променя для довжин хвиль збудження та пригнічення. Ці властивості роблять їх кращими для компактних інтегрованих систем мікроскопії STED. Отримані результати можуть слугувати орієнтиром для вибору та оптимізації волокон для візуалізації з високою роздільною здатністю.

Ключові слова: оптичні волокна, оптичні вихори, LP-моди, STED-мікроскопія